Ti^{IV} Uptake and Release by Human Serum Transferrin and Recognition of Ti^{IV}-Transferrin by Cancer Cells: Understanding the Mechanism of Action of the Anticancer Drug Titanocene Dichloride†

Maolin Guo,‡ Hongzhe Sun,§ Harry J. McArdle,|| Lorraine Gambling,|| and Peter J. Sadler*,‡

Department of Chemistry, University of Edinburgh, Edinburgh EH9 3JJ, U.K., Department of Chemistry, University of Hong Kong, Pokfulam Road, Hong Kong, P. R. China, and Division of Nutrition, Pregnancy and Development, Rowett Research Institute, Greenburn Road, Aberdeen AB21 9SB, U.K.

Received April 10, 2000

ABSTRACT: The organometallic anticancer agent titanocene dichloride, Cp_2TiCl_2, is now in phase II clinical trials as an anticancer drug, but its mechanism of action is poorly understood. We show here that the interactions of Cp_2TiCl_2 with human serum transferrin (hTF) and that of Ti_2-hTF with adenosine triphosphate (ATP) have characteristics that could allow transferrin to act as a mediator for titanium delivery to tumor cells. Such reactions may therefore be important to the anticancer activity of this new class of drugs. Cp_2TiCl_2 reacts rapidly with human apo-transferrin under physiological conditions (100 mM NaCl, 25 mM bicarbonate, and 4 mM phosphate, pH 7.4) with carbonate as a synergistic anion. The Cp ligands are released from the drug. Two-dimensional [^{1}H, ^{13}C] NMR studies of ϵ-[^{13}C]Met-hTF show that Ti^{IV} loads the C-lobe first followed by the N-lobe and binds in the specific Fe^{III} sites. The protein conformational changes induced by Ti^{IV} appear to be similar to those induced by Fe^{III}. Carbonate can act as a synergistic anion in Ti_2-hTF but does not appear to be essential. A specific Ti^{IV}-hTF adduct is formed even in the absence of bicarbonate. When the pH of Ti_2-hTF solutions is lowered, no Ti^{IV} is released at the endosomal pH of ca. 5.0−5.5, but one Ti^{IV} dissociates between pH 4.5−2.0. In contrast, in the presence of 1 mM ATP, all Ti^{IV} is readily released from both lobes when the pH is lowered from 7.0 to 4.5. Moreover, Fe^{III} displaces Ti^{IV} rapidly from the C-lobe of Ti_2-hTF (<5 min) but only slowly (days) from the N-lobe. Thus, the species Fe_CTi_N-hTF might also provide a route for Ti^{IV} entry into tumor cells via the transferrin receptor. Ti_2-hTF effectively blocked cell uptake of radiolabeled ^{59}Fe-hTF into BeWo cells, a human placental choriocarcinoma cell line in culture. These results imply that titanium transferrin might be recognized by the transferrin receptor and be taken up into cancer cells.

Two classes of Ti^{IV} complexes, organometallic biscyclopentadienyl titanium^{IV} complexes and bis(β-diketonato)-Ti^{IV} complexes, have been shown to exhibit high antitumor activities against a wide range of murine and human tumors, with less toxic side effects than cisplatin (*1*, *2*). Titanocene dichloride (Cp_2TiCl_2, Cp = η^5-C_5H_5) is currently in phase II clinical trials as an anticancer agent (*3*−*5*). Titanocene dichloride significantly overcomes cisplatin resistance in ovarian carcinoma cell lines (*6*) and also exhibits pronounced antiviral, antiinflammatory and insecticidal activities (*7*). In addition, some Ti^{IV} complexes show pronounced antibacterial activity (*8*−*10*), and ^{45}Ti is potentially useful as a radiopharmaceutical (*11*). However, in contrast to platinum-based anticancer drugs (*12*), the biological chemistry and mechanism of action of titanium compounds are poorly understood (*1*, *2*, *13*). Attack on cellular nucleic acids is believed to be crucial for the antitumor activity of Cp_2TiCl_2, which inhibits DNA synthesis rather than RNA and protein synthesis, and titanium accumulates in nucleic acid-rich regions of tumor cells after in vivo or in vitro administration (*7*, *14*, *15*). However, unlike cisplatin, Ti^{IV} does not bind strongly to DNA bases at physiological pH but forms strong complexes with nucleotides only at pH values below 5 (*16*). This and the finding that the vanadium and molybdenum analogues fail to form stable complexes with DNA under physiological conditions, raise doubts that nucleic acids are the predominant target (*13*, *17*, *18*). Efforts to identify the biologically active species have been largely unsuccessful due to the rapid hydrolysis of Ti^{IV} complexes at neutral pH and the precipitation of polymeric hydrolysis products (*2*, *19*).

Recently, we reported our preliminary finding that Ti^{IV} binds strongly to the serum transport protein transferrin (*20*, *21*). This was subsequently confirmed by other workers (*22*) and suggests that transferrin may mediate the uptake of Ti from the anticancer drug into cells. Transferrin is an 80-kDa glycoprotein present in blood plasma at a concentration of ca. 35 μM. It has two specific Fe^{III} binding sites, one in the N-lobe and one in the C-lobe, each providing ap-

† We thank the Committee of Vice-Chancellors and Principals for an ORS award and the University of Edinburgh for a Scholarship for M.G. The work was funded by the Engineering and Physical Sciences Research Council and Biotechnology and Biological Sciences Research Council.

* To whom correspondence should be addressed. Phone (+44) 131 650 4729. Fax (+44) 131 650 6452. E-mail: p.j.sadler@ed.ac.uk.

‡ University of Edinburgh.

§ University of Hong Kong.

|| Rowett Research Institute.

10.1021/bi000798z CCC: $19.00
Published on Web 07/27/2000

Chart 1

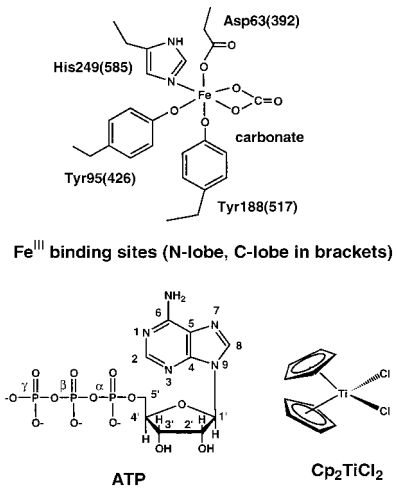

proximately octahedral coordination from two Tyr, His, Asp, and bidentate carbonate (synergistic anion) ligands (see Chart 1). The major receptor recognition sites on hTF are thought to be localized on the C-lobe (*23*−*26*), supported by the recent X-ray crystal structure of the human transferrin receptor (*25*). Transferrin in human serum is only 30% saturated with iron, and the vacant sites can bind other metal ions (*35*, *36*). It has been suggested that transferrin can act as a natural carrier for anticancer metal ions (*36*) as well as other chemotherapeutic drugs (*26*), since there are high levels of transferrin receptors on the surface of tumor cells (*27*−*30*), possibly due to their increased requirement of iron for metabolism, growth, and development. Indeed, it has been suggested that transferrin is responsible for the transport and delivery of metal ions such as $^{67}Ga^{III}$ and Ru^{III} to cancer cells (*31*, *32*). Transferrin takes up Fe^{III} at pH 7.4 and delivers it to cells via receptor-mediated endocytosis (*33*). The general features of this process are now well-understood (*34*−*36*). First, Fe^{III} binds to apo-hTF and induces a major conformational change of the protein, from the lobe-open to the lobe-closed form. Then, the iron-saturated holo-hTF binds to the specific transferrin receptors on the cell surface and is internalized by clathrin-coated vesicles into endosomes. Here the pH is mildly acidic (pH ca. 5.0−5.5), and Fe^{III} is released from the transferrin. ATP is a possible direct Fe^{III} acceptor from transferrin and a major Fe^{III} carrier inside cells (*34*, *37*).

We report here a detailed study of uptake of Ti^{IV} from the anticancer agent Cp_2TiCl_2 by human transferrin at blood plasma pH values, release of bound Ti^{IV} to ATP at cellular endosomal pH values, and displacement of Ti^{IV} by Fe^{III}, as well as uptake of Ti_2-hTF into BeWo placental cancer cells. These studies may shed light on how titanium anticancer complexes are activated in vivo, as well as on the rational design of more active and less toxic metallodrugs.

MATERIALS AND METHODS

Materials. Apo-hTF was purchased from Sigma (catalog no. T0519) and washed three times with 0.1 M KCl to remove low molecular mass impurities using Centricon 30 ultrafilters (Amicon). Titanocene dichloride was purchased from Arcos Chemical Co. and was used in all the experiments as a freshly prepared DMSO/saline (0.1 M NaCl; 1/9,v/v) solution at 277 K, as reported for in vivo experiments (*14*, *15*). This stock solution was ca. 10−20 mM and was used within 5 h. 5′-Adenosine triphosphate disodium salt (ATP) was obtained from Aldrich Chemical Co. and was used as a freshly prepared aqueous solution. The purity was verified by ^1H and ^{31}P NMR spectroscopy. $NaHCO_3$ (Aldrich), nitrilotriacetic acid (H_3NTA, Aldrich), Hepes (Aldrich), $NaH^{13}CO_3$ (MSD isotopes, >99% enriched), and $^{59}FeCl_3$ (Amersham, in 0.1 M HCl) were used as received. ^{59}Fe-hTF was prepared by incubating apo-hTF with $^{59}FeCl_3$ in the presence of $NaHCO_3$. Recombinant ϵ-[$^{13}CH_3$]Met-hTF was supplied by Professor R. C. Woodworth and Dr. A. B. Mason (University of Vermont) and was prepared as previously described (*38*, *39*). All other chemicals were reagent-grade and were used as received. For all the UV experiments, a freshly prepared physiological buffer was used with final concentrations of 4 mM NaH_2PO_4, 100 mM NaCl, and 25 mM $NaHCO_3$ (pH 7.4).

A solution of [$Fe(NTA)_2$] was prepared from the iron atomic absorption standard solution and 2 mol equiv of H_3-NTA. The pH was slowly raised to 5.5 with microliter amounts of NaOH (1 M), and this solution was then diluted to 9.0 or 1.8 mM.

UV−*Vis Spectroscopy.* Apo-hTF solutions were prepared by diluting aliquots of a stock apo-hTF solution to ca. 2.5 × 10^{-5} M with physiological buffer, pH 7.4. The hTF concentrations were determined spectrophotometrically using ϵ_{280} 93 000 $M^{-1}cm^{-1}$ (*40*). UV difference spectra after addition of Cp_2TiCl_2 to apo-hTF were recorded immediately and at different time intervals. For titration experiments, aliquots of Cp_2TiCl_2 (0.5−10 μL) were added, and the solution was left to equilibrate at 298 K for 30 min. The binding or release of Ti^{IV} was monitored by the increase or decrease in absorbance at 321 nm. All the UV experiments were performed with 1-cm cuvettes on a computer-controlled Shimadzu UV-1000 spectrometer with temperature control at 298 or 310 K.

NMR Spectroscopy. Apo-transferrin was dissolved in 0.1 M KCl in D_2O/H_2O (10%/90%) containing 10 mM $NaHCO_3$. The pH was adjusted to 7.4 ± 0.1, when necessary, using NaOH and HCl (0.1 M). The pH* values (meter readings) of NMR solutions were recorded before and after NMR measurements.

^1H NMR spectra were recorded on a Bruker DMX 500 spectrometer at 500 MHz, using 0.6 mL of hTF solution (ca. 0.8 mM) in 5-mm tubes at 298 K, using ca. 1000 transients, 6 μs (50°) pulses, 1.8 s recycle time, 16 384 data points, and water suppression via presaturation. The chemical shift reference for ^1H was sodium trimethylsilyl-d_4-propionate (TSP) via endogenous formate (8.465 ppm, pH* > 7). Resolution enhancement of the spectra was achieved by processing the free induction decays with a combination of unshifted sine-bell and exponential functions (line broadening of 1.5−20 Hz) on a Silicon Graphics computer using XWIN NMR software.

Proton-decoupled ^{13}C and ^{31}P NMR spectra were recorded on a Bruker DMX 500 spectrometer operating at 125 and 202 MHz, respectively. Typically, 30 000 (^{13}C) or 1000−2000 (^{31}P) transients were collected using 50° pulses, relaxation delay 2 s, and 16 384 data points. The ^{13}C reference was external TSP, and for ^{31}P was external 85%

H_3PO_4. The spectra were processed using exponential functions (line-broadening of 5−20 Hz).

NMR samples of ϵ-[^{13}C]Met-hTF (ca. 0.26 mM) were prepared in 0.1 M KCl in D_2O/H_2O (30%/70%), and pH values were adjusted to 7.4 ± 0.1 using NaOH or HCl. Sodium bicarbonate in D_2O (0.25 M) was added to transferrin solutions to give a concentration of 10 mM. After addition of Cp_2TiCl_2 to protein samples to give drug/protein mol ratios of up to 2:1, the pH was readjusted to 7.4 ± 0.1, and the samples were left 30 min at 298 K for equilibration.

2D [^{1}H, ^{13}C] HSQC spectra (*41*) were acquired on a Bruker DMX 500 spectrometer at 298 K. The sequence was optimized for $^1J(^1H\text{-}^{13}C) = 136$ Hz, and 16−32 transients were acquired using 2048 data points in the f2 dimension (^{1}H), 32−64 increments of t_1, ^{13}C frequency width of 3000 Hz (sw1), and relaxation delay of 1.6 s, giving a total of ca. 30 min to 1 h for the acquisition of each spectrum. The GARP-1 sequence (*42*) was used to decouple ^{13}C. After zero-filling to 2048 × 512 points, unshifted-Gaussian functions were used for processing. The residual water signal was suppressed by a combination of presaturation and pulsed-field gradients. Peaks were referenced to TSP via the ϵ-CH_3 peak of L-methionine (external, 15.14 ppm) for ^{13}C and via formate (8.465 ppm, present as a minor impurity) for ^{1}H.

Inductively Coupled Plasma Atomic Emission Spectrometry (ICP-AES). This was performed on a Thermo Jarrell Ash IRIS spectrometer using standard methods. Metal-loaded protein was purified by using Centricon 30 (Amicon) ultrafilters and washing three times with ultrapure water followed by ultrafiltration after each washing. The final protein solution was diluted with ultrapure water, and titanium and iron contents were measured without digestion of the sample.

pH Measurements. The pH values of the solutions were adjusted with HCl or NaOH (DCl or NaOD for samples in D_2O solution) and determined using a Corning 240 pH meter equipped with an Aldrich micro combination electrode, calibrated with Aldrich buffer solutions at pH 4, 7, and 10. The pH meter readings for D_2O solutions are recorded as pH* values, i.e., uncorrected for the effect of deuterium.

Bicarbonate-Free Experiments. All the solutions were freshly prepared using ultrapure water and were bubbled thoroughly with high-purity helium to remove residual CO_2. Anaerobic UV cuvettes were used to prevent CO_2 contamination from the air. Similar experiments in the presence of $NaHCO_3$ were also carried out for comparison.

Cell Culture Experiments. BeWo cells were cultured to 80% confluence in Ham's F12 medium plus 10% fetal calf serum, with glutamine, penicillin, and streptomycin. The cells were washed three times with balanced salt solution (BSS, 136 mM NaCl, 5 mM KCl, 1 mM $CaCl_2$, 1 mM $MgCl_2$, and 18 mM Hepes, pH 7.4) and incubated in balanced salt solution containing 0.5 μM ^{59}Fe-hTF for 1 h at 310 K in the presence or absence of competing metal transferrin complexes, at increasing molar ratios. Following incubation, the cells were washed three times with balanced salt solution and incubated with Pronase (1 mg/mL) for 30 min at 277 K. They were aspirated from the plate into Eppendorf tubes and centrifuged at 14000*g* for 1 min. The supernatant was removed and counted, representing surface-bound ^{59}Fe. The pellet was resuspended in 1 mL BSS and sonicated, and 100 μL was removed for DNA analysis. The remaining 900 μL was counted representing intracellular ^{59}Fe (*43*). All values were calculated as cpm/μg DNA and are the mean ± SEM of four experiments, each performed in triplicate. DNA was analyzed using Hoechst dye as previously described (*43*).

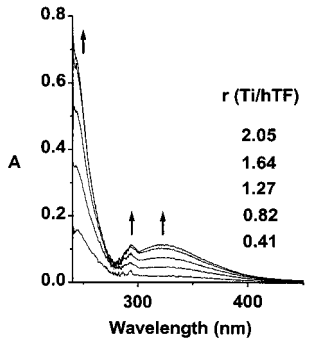

FIGURE 1: Reaction of Cp_2TiCl_2 with apo-hTF gives rise to new bands in the UV difference spectrum after addition of various mole equivalents of Cp_2TiCl_2. Conditions: 25 μM apo-hTF in 100 mM NaCl, 25 mM HCO_3^-, and 4 mM NaH_2PO_4, pH 7.4, 298 K. Ratio (Ti/hTF) from bottom to top: 0.41, 0.82, 1.27, 1.64, and 2.05.

RESULTS

Reactions of human serum transferrin, recombinant isotopically labeled human transferrin (ϵ-[^{13}C]Met-hTF with > 95% ϵ-$^{13}CH_3$ enrichment at all nine Met residues) with the anticancer complex Cp_2TiCl_2, Ti^{IV} release to ATP, and displacement of Ti^{IV} by Fe^{III} were studied by UV−Vis spectroscopy, ICP-AES spectrometry, and one-dimensional ^{1}H,^{13}C, ^{31}P, and 2D [^{1}H, ^{13}C] NMR spectroscopy under physiologically relevant conditions.

Uptake of Ti^{IV} by apo-hTF from Anticancer Drug Cp_2TiCl_2 under Physiologically Relevant Conditions. Reactions of the anticancer drug Cp_2TiCl_2 with human serum apo-transferrin in physiological buffer (100 mM NaCl, 4 mM phosphate, and 25 mM bicarbonate, pH 7.4) were studied initially using UV−Vis spectroscopy. When 2 mol equiv of Cp_2TiCl_2 was added to an aqueous solution of apo-hTF (2.4×10^{-5} M) at 310 K, two new sharp bands at 242 and 295 nm and a new broad band at 321 nm appeared immediately in the difference spectrum and increased in intensity over a period of 5 min. There was little further change in the spectrum over a period of 24 h (data not shown).

A titration to investigate the stoichiometry of Ti^{IV} binding was performed under similar conditions but at 298 K. Selected UV difference spectra at equilibrium are shown in Figure 1. A plot of ΔA_{321} against the molar ratio (r) of Cp_2TiCl_2 to apo-hTF is shown in Figure 2. It can be seen that with the increase of r, the three UV bands near 242, 295, and 321 nm increase in intensity and reach a plateau at $r = 2$, which suggests that two Ti^{IV} ions bind strongly to transferrin (i.e., one in each lobe). The value of the extinction coefficient for the broad band at 321 nm is 4830 $M^{-1}cm^{-1}$ based on protein concentration. The resulting yellow Ti_2-hTF solution was stable at ambient temperature for several weeks.

^{1}H NMR studies were carried out to investigate the structural changes in hTF induced by reactions with Cp_2TiCl_2. Aliquots of a solution of Cp_2TiCl_2 (0−2 mol equiv, freshly prepared in DMSO-d_6/saline, 1/9, v/v) were added to a solution of apo-hTF in 0.1 M KCl (D_2O/H_2O, 10/90%) containing 10 mM bicarbonate, pH 7.4. ^{1}H NMR spectra of

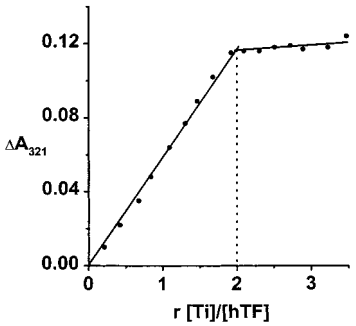

FIGURE 2: Titration curve for the reaction of Cp_2TiCl_2 with apo-hTF. Increase in intensity of the LMCT band at ca. 321 nm is plotted against the ratio [Ti]/[hTF] (*r*). Conditions: as Figure 1.

hTF are complicated by the overlap of a large number of resonances from this large molecule (80 kDa). However, some regions of the ^{1}H NMR spectrum are sensitive to metal binding to the specific iron sites of the protein (*44*). The region near 2 ppm contains resonances due to the *N*-acetyl groups of the NAcGlc and NAcNeu residues in each of the two biantennary glycan chains attached to Asn-413 and Asn-611 in the C-lobe of the protein (*39*, *45*, *46*). The high-field region (0.5 to −1 ppm) consists mainly of ring-current shifted resonances, including those from groups in hydrophobic patches near the specific metal binding sites in both the N-lobe and the C-lobe of the protein (*47*). The 500-MHz ^{1}H NMR spectrum of the *N*-acetyl region is shown in Figure S1 (in Supporting Information). After addition of the first mole equivalent of Cp_2TiCl_2, two new sharp peaks appeared at 2.07 and 2.03 ppm, together with a broad weak peak at 2.10 ppm. No further changes occurred in this region on addition of the second equivalent of Cp_2TiCl_2. The changes that occurred in the high-field region of the 500-MHz ^{1}H NMR spectrum were similar to those observed previously for reactions of Ti^{IV}-citrate with apo-hTF (*20*).

^{1}H NMR studies were also carried out to investigate whether the Cp ligands are displaced during the reaction of Cp_2TiCl_2 with hTF. Ti^{IV}-bound Cp exhibits a singlet at 6.42 ppm at neutral pH, while released Cp (CpH) shows two multiplets at 6.57 and 6.62 ppm and a weak multiplet at 2.95 ppm (*19*). The 500-MHz ^{1}H NMR spectra recorded over the period 10−40 min during reaction of 1 mol equiv of Cp_2TiCl_2 with apo-hTF in the presence of 10 mM bicarbonate at pH* 7.4, 298 K, are shown in Figure S2 (in Supporting Information). It can be clearly seen that a strong singlet for Ti^{IV}-bound Cp at 6.42 ppm is present after 10 min and that two broad peaks at 6.57 and 6.62 ppm are already discernible. The latter peaks continued to increase in intensity at the expense of the peak at 6.42 ppm. After 30 min, the peak at 6.42 ppm had nearly disappeared, and the peaks at 6.57 and 6.62 ppm had attained their maximum intensities. With the addition of a second mole equivalent of Cp_2TiCl_2, similar changes in intensity of the CpH peaks were observed with time (data not shown).

^{13}C NMR studies were carried out to investigate whether the binding of Ti^{IV} to hTF also involved concomitant binding of carbonate as synergistic anion. The carbonyl region of a 125 MHz ^{13}C NMR spectrum of apo-hTF in the presence of 4 mol equiv of $H^{13}CO_3^-$ (4 mM, enriched to > 99% in ^{13}C) and after addition of 2 mol equiv of Cp_2TiCl_2 is shown in Figure S3 (in Supporting Information). In the absence of Cp_2TiCl_2, a sharp peak at 161.1 ppm due to $H^{13}CO_3^-$ was observed, together with a broad envelope at 173−183 ppm corresponding to the backbone and side-chain carbonyls of apo-hTF (natural abundance ^{13}C) (*48*). In the presence of Cp_2TiCl_2, the peak due to free $H^{13}CO_3$ decreased in intensity markedly, and a new peak assignable to Ti-CO_3-hTF appeared at 166.5 ppm. This peak is weak and has a chemical shift comparable with that for hTF loaded with other diamagnetic metals (such as Ga^{3+}, Bi^{3+}, Co^{3+}) and had disappeared when the spectrum was recorded 3 weeks later.

Ti^{IV} Binding to Apo-hTF under Bicarbonate-Free Conditions. To investigate whether carbonate as synergistic anion is essential for Ti^{IV} binding to apo-hTF, comparative UV−Vis and ^{1}H NMR experiments were performed in the absence or presence of bicarbonate. In the absence of bicarbonate, the reaction of 2.0 mol equiv of Cp_2TiCl_2 with apo-hTF (30 μM) in 10 mM Hepes buffer, pH 7.4, 298 K, give rise to three new bands in the UV−Vis difference spectrum at ca. 242, 295, and 315 nm, which increased in intensity over a period of 1 h. Similar UV−Vis changes were observed in the presence of 5 mM bicarbonate and at the same apo-hTF concentration, but the reaction was faster (0.5 h), and the intensities of the bands were lower at equilibrium (ca. 26% lower at 315 nm). However, when $NaHCO_3$ (5 mM final) was introduced into the Ti_2-hTF solutions formed under bicarbonate-free conditions, the bands decreased in intensity markedly over a period of 4 h, and the final UV−Vis difference spectrum was nearly identical to that for Ti_2-hTF formed in the presence of bicarbonate.

To investigate possible structural differences between Ti_2-hTF adducts formed in the absence and in the presence of bicarbonate, ^{1}H NMR experiments were performed. When Cp_2TiCl_2 was added into the apo-hTF solution (0.7 mM), a yellow color developed. However, the changes in NMR peaks in the absence of bicarbonate were quite different from those in the presence of bicarbonate (vide infra). In the glycan *N*-acetyl region near 2 ppm, there was little change when 1.0 or 2.0 mol equiv of Cp_2TiCl_2 was added (data not shown) in the absence of bicarbonate, in contrast to the marked changes in the presence of bicarbonate (see Figure S1 in the Supporting Information). These peaks remained unchanged even when 10 mM $NaHCO_3$ was introduced into the solution. In the high field region (see Figure S4 in the Supporting Information), the changes to peaks in the absence of bicarbonate were also different from those in the presence of bicarbonate when 1.0 or 2.0 mol equiv of Cp_2TiCl_2 was added to the apo-hTF solution. When 10 mM of bicarbonate (^{13}C-enriched) was introduced after the reaction of Cp_2TiCl_2 and apo-hTF in the absence of bicarbonate, some peak changes in the high field region occurred slowly, but the final spectrum was not identical to that for Ti_2-hTF formed in the presence of bicarbonate (see Figure S4). A ^{13}C NMR spectrum recorded after introducing $NaH^{13}CO_3$, contained a small peak at 166.5 ppm, but this disappeared 4 days later (data not shown).

Order of Lobe Loading of apo-hTF with Ti^{IV}. 2D [^{1}H, ^{13}C] NMR spectra of recombinant nonglycosylated human transferrin with > 95% ϵ-$^{13}CH_3$ enrichment at all nine Met residues (for locations, see Figure S5 in Supporting Information) were obtained using inverse detection techniques (*49*, *50*). When 0.65 mol equiv of Cp_2TiCl_2 was added to recombinant apo-hTF at pH 7.4 in the presence of 10 mM $NaHCO_3$, the cross-peak for Met-464 in the C-lobe of the

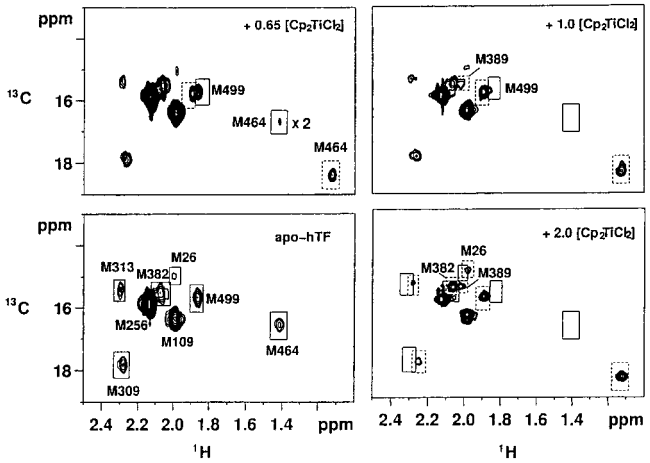

FIGURE 3: Detection of the order of lobe loading of hTF with Ti^{IV}. 2D [^{1}H,^{13}C] HSQC spectra of ϵ-$^{13}CH_3$-Met-hTF (0.26 mM in 0.1 M KCl, and 10 mM bicarbonate, pH* 7.4) and after addition of 0.65, 1.0, and 2.0 mol equiv of Cp_2TiCl_2. Solid boxes indicate initial peaks, and dotted boxes show new peaks. There are specific shifts of cross-peaks for the C-lobe residues Met-464 and Met-499 on binding to the first equiv of Cp_2TiCl_2 and N-lobe residues Met-309 and Met-313 on binding the second equiv of Cp_2TiCl_2. Assignments are based on refs *39* and *50*.

protein decreased markedly in intensity (Figure 3), and a new strong peak shifted ca. 2 ppm downfield in the ^{13}C dimension and ca. 0.2 ppm upfield in the ^{1}H dimension appeared concomitantly. The cross-peak for C-lobe Met-499 (1.86/15.65 ppm) split into two peaks with the new peak appearing slightly to low field in both ^{13}C and ^{1}H dimensions. With 1.0 mol equiv of Cp_2TiCl_2 present, the original cross-peaks for Met-464 and Met-499 had disappeared almost completely, and the new peaks at 1.12/18.32 ppm and 1.89/15.68 ppm had increased in intensity; similarly, the cross-peak for Met-499 had almost completely shifted to its new position. Also, a cross-peak assignable to Met-389, which was not observed for the apo-protein, appeared after addition of 1.0 equiv of Cp_2TiCl_2 (Figure 3). When the second mol equiv of Cp_2TiCl_2 was added, there was no further change to the cross-peaks for the C-lobe Met residues, but shifts were observed for the cross-peaks of the N-lobe residues Met-26, Met-309, and Met-313.

pH-induced Ti^{IV} Release from Ti_2-hTF. The pH-dependent properties of Ti_2-hTF (obtained from the reactions of Cp_2TiCl_2 with apo-hTF in physiological buffer) were investigated over the pH range of 2 to 10 by introducing aliquots of HCl or NaOH (0.5−3.0 M), and the absorbance at 321 nm (ligand-to-metal charge-transfer LMCT band) was then measured after incubation at 298 K for 1 h. No absorbance change at 321 nm was evident over the pH range of 5.0 to 9.5 (see Figure 4), suggesting that Ti_2-hTF is stable over this pH range. Below pH 5, the absorbance at 321 nm decreased and plateaued to ca. 53% of its initial value by pH 2, implying cleavage of Ti^{IV}-tyrosinate bonds in the protein. Ti_2-hTF was stable at alkaline pH with a small decrease in A_{321} only at pH > 9.5 (Figure 4).

Ti^{IV} Release from Ti_2-hTF in the Presence of ATP. In the presence of 1 mM ATP, the A_{321} value for Ti_2-hTF decreased sharply over the pH range 7.4 to 5.0 and by pH 4.5 was the same as that of apo-hTF in the presence of the same concentration of ATP (Figure 4). This suggests that Ti^{IV} is completely released from Ti_2-hTF under these conditions.

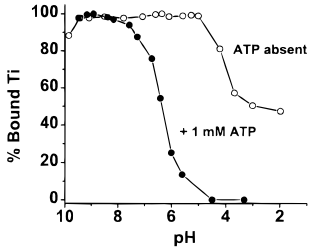

FIGURE 4: pH-dependent profile of Ti^{IV} release from Ti_2-hTF and the effect of ATP. Conditions: 20 μM Ti_2-hTF in 100 mM NaCl, 25 mM HCO_3^-, and 4 mM NaH_2PO_4, 298 K, in the absence (open circles) or presence (closed circles) of 1 mM ATP, as monitored by the Ti^{IV}-tyrosinate charge-transfer band at 321 nm.

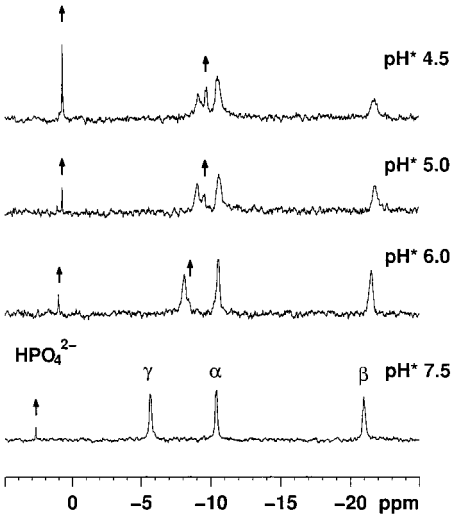

FIGURE 5: Effect of Ti_2-hTF on the 202-MHz $^{31}P\{^1H\}$ NMR spectrum of ATP at different pH values. Conditions: ATP/Ti_2-hTF = 2:1, 1.0 mM Ti_2-hTF in 0.1 M KCl, 70% H_2O/30% D_2O, spectra recorded after equilibration at 298 K for 0.5 h.

This contrasted with the partial release of Ti^{IV} from Ti_2-hTF in acidic solutions in the absence of ATP.

A $^{31}P\{^1H\}$ NMR pH titration was carried out to investigate further the role of ATP (see Chart 1) in facilitating Ti^{IV} release from Ti_2-hTF. A solution of purified Ti_2-hTF in the presence of 2 mol equiv of ATP was titrated over the pH range 7.5 to 4.5 in ca. 0.5 pH unit steps, each equilibrated at 298 K for ca. 30 min before the $^{31}P\{^1H\}$ spectrum was recorded. A similar pH titration of ATP at the same concentration but in the absence of Ti_2-hTF was also studied for comparison. The ^{31}P NMR spectrum of ATP alone at pH 7.0 shows doublets at −6.97 and −10.38 ppm and a triplet at −21.20 ppm, assignable to the γ, α, and β phosphate groups, respectively (*51*). These shifts changed only slightly over the pH range of 8.0 to 4.0, and no hydrolysis was observed. However, in the presence of Ti_2-hTF, a new $^{31}P\{^1H\}$ peak assignable to inorganic phosphate (*16*) appeared at 2.72 ppm even at pH 7.5, as shown in Figure 5. This peak continued to increase in intensity and shift to higher field as the pH was lowered. Also, at pH 6.0, a new $^{31}P\{^1H\}$ doublet appeared to high field of the γ phosphate signal and continued to increase in intensity at the expense of the γ phosphate signal as the pH was lowered. However, there was little change in the α phosphate peak. In the ^{1}H NMR spectrum, peaks for H8, H2, and H1′ of ATP gradually lost intensity when the pH was lowered and had almost disappeared by pH* 4.5.

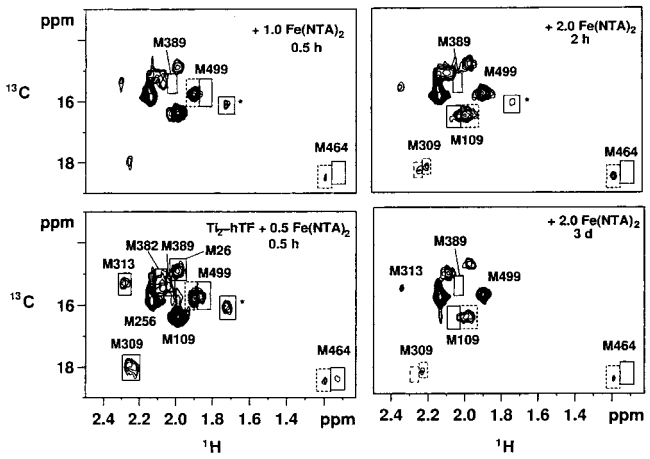

FIGURE 6: Determination of the order of displacement of Ti^{IV} from the N- and C-lobes of Ti_2-hTF by Fe^{III}. 2D [^{1}H,^{13}C] HSQC spectra of ϵ-[$^{13}CH_3$]Met-Ti_2-hTF (0.26 mM in 0.1 M KCl, and 10 mM bicarbonate, pH* 7.4) after addition of 0.5 (0.5 h), 1.0 (0.5 h), 2.0 (2 h) and 2.0 (3 days) mol equiv of $Fe(NTA)_2$ (equilibrated for the periods specified). Solid boxes indicate initial peaks, and dotted boxes show new peaks. The spectrum of Ti_2-hTF alone is shown in Figure 3. Specific shifts of cross-peaks for the C-lobe residues Met-464 and Met-499 on binding to the first mole equivalent of Fe^{III} and N-lobe residues Met-309 and Met-109 on binding the second mole equivalent of Fe^{III} are notable. An additional cross-peak marked with an asterisk (*) also appeared during the course of the titration but had disappeared by the time the final spectrum was recorded.

Fe^{III} Displacement of Ti^{IV} from Ti_2-hTF. When 2.5 mol equiv of $Fe(NTA)_2$ was added to a solution of Ti_2-hTF (physiological buffer, pH 7.4, 298 K), a new broad band in the visible region centered at ca. 465 nm appeared in the difference spectrum and gradually increased in intensity over a period of about 30 h (Figure S6 in Supporting Information). The reaction appeared to proceed in two phases: a first fast phase lasting about 7 min and accounting for ca. 50% of the total increase in intensity at 465 nm, and a second slower phase lasting for about 30 h, which accounted for the remaining 50% increase in intensity at 465 nm. The second phase itself appeared to consist of two steps with the initial stage lasting from 7 min to ca. 1 h. Increases in intensity at $>$438 nm were accompanied by decreases in intensity at $<$438 nm. An isobestic point was observed at 438 nm during this period, indicating a two-state mechanism. The second step lasted for up to 30 h with increases in intensity around 472 nm. Also, the absorption maximum at 465 nm, which was seen during the first phase, shifted to 472 nm during the second phase.

The order of displacement of Ti^{IV} from the two lobes by Fe^{III} was established by 2D [^{1}H, ^{13}C] HSQC NMR studies using ϵ-$^{13}CH_3$-Met-labeled recombinant human transferrin. To fully load the protein with Ti^{IV}, 2.5 mol equiv of Cp_2TiCl_2 was added to the labeled apo-protein in the presence of 10 mM of $NaHCO_3$. A yellow color developed quickly, and the 2D [^{1}H, ^{13}C] HSQC NMR spectrum was identical to that in Figure 3, indicating formation of Ti_2-hTF. Aliquots of $Fe^{III}(NTA)_2$ solution were added to the Ti_2-hTF solution at pH 7.4 to give Fe/hTF mol ratios of 0.5:1 to 2.0:1 (in steps of 0.5 mol equiv, with equilibration for 30 min at 298 K before recording the spectrum). The color of the solution changed from light yellow to brown red during the additions. As shown in Figure 6, the addition of the first 0.5 mol equiv of Fe^{III} to Ti_2-hTF led to a dramatic decrease in intensity of the cross-peaks for Met-464 and Met-499 of Ti_2-hTF and was accompanied by the appearance of two new peaks at slightly lower field in the ^{1}H dimension. With 1.0 mol equiv of Fe^{III} present, the original cross-peaks for Met-464 and Met-499 of Ti_2-hTF completely disappeared as did the cross-peak for Met-389. No shifts were observed for the cross-peaks of the Met residues in the N-lobe although the peaks Met-309 and Met-313, which are in the interlobe contact region, decreased in intensity (Figure 6). With 1.5 and 2.0 mol equiv of Fe^{III} present, no further changes to these C-lobe peaks was observed, but shifts of the cross-peaks for Met residues in the N-lobe, Met-109, Met-309, and Met-313 developed over a period of several hours: a 2D HSQC NMR spectrum recorded 0.5 h after addition of 1.5 equiv of $Fe(NTA)_2$ revealed that Met-313 had split into two peaks, but there was little change in the other cross-peaks (data not shown). However, 2 h after addition of 2.0 mol equiv of $Fe(NTA)_2$, new cross-peaks were observed for Met-309 and Met-109, shifted to slightly lower field in the ^{1}H dimension (Figure 6). The above sample (with 2.0 mol equiv of Fe^{III} present) was left at ambient temperature for 3 days, at which time some white precipitate was visible in the solution. The 2D [^{1}H, ^{13}C] HSQC NMR spectrum at this time was almost identical to that observed for Fe_2-hTF (*49*). An interesting feature in Figure 6 is the presence of an additional ^{1}H/^{13}C cross-peak at 1.72/16.03 ppm (marked by *), which is not present in the spectra of either Ti_2-hTF or the final protein Fe_2-hTF. It was most intense during the addition of the first equivalent of Fe^{III} and had disappeared by the time the final spectrum was recorded.

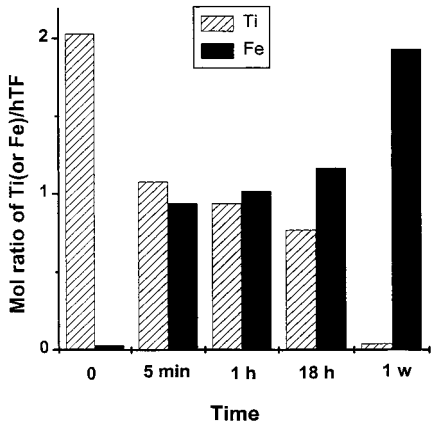

FIGURE 7: Time dependence of the displacement of Ti^{IV} from Ti_2-hTF by Fe^{III}. Metal contents were measured by ICP-AES. Note the rapid displacement of one Ti^{IV} by Fe^{III} followed by a much slower displacement of the second Ti^{IV}.

ICP-AES Studies. To further confirm the displacement of Ti^{IV} by Fe^{III}, the metal content of hTF at various stages of the titration of Ti_2-hTF (19.4 μM) with $Fe(NTA)_2$ (2.5 mol equiv) in physiological buffer (pH 7.4) was determined by inductively coupled plasma atomic emission spectrometry (ICP-AES). After incubation at ambient temperature (ca. 293 K) for various times, the sample was ultrafiltered, and the protein was purified by washing three times with ultrapure water followed by ultrafiltration (Centricon 30). The metal (Ti and Fe) content was measured without digestion of the protein. The results are shown in Figure 7. For Ti_2-hTF without added $Fe(NTA)_2$, the Ti/hTF ratio was determined to be 2.03, and Fe/hTF ratio was determined to be 0.03. After

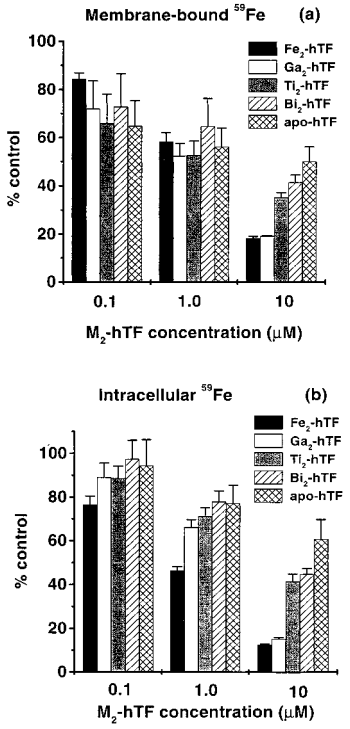

FIGURE 8: Effect of increasing concentration of metal transferrins on uptake of ^{59}Fe from ^{59}Fe-hTF by BeWo cells. Cells were incubated with 0.5 μM ^{59}Fe-hTF in the presence or absence of 0.1, 1, or 10 μM metal-transferrins (Fe_2-hTF, Ga_2-hTF, Ti_2-hTF, Bi_2-hTF) and apo-hTF. Data are expressed as a percentage of untreated control cells (100%). (a) Membrane-bound ^{59}Fe; (b) intracellular ^{59}Fe.

5 min of reaction of Fe^{III} with Ti_2-hTF, the Ti/hTF ratio was 1.08 and Fe/hTF ratio was 0.94, i.e., nearly half of the protein-bound Ti^{IV} had been displaced by Fe^{III}. One hour later, the Ti/hTF ratio was 0.94 and Fe/hTF ratio was 1.02; 18 h later, the Ti/hTF ratio was 0.77 and Fe/hTF ratio was 1.17, confirming a slow displacement of Ti^{IV} by Fe^{III} during the second phase. One-week later, a small amount of white precipitate developed, and only the supernatant was used for metal determinations. This gave a Ti/hTF ratio of 0.04 and a Fe/hTF ratio of 1.93, indicating that Ti^{IV} had now been completely displaced from Ti_2-hTF by Fe^{III}.

Cell Uptake Studies. To investigate whether Ti_2-hTF can be recognized by transferrin receptors and subsequently taken up into cells, Ti_2-hTF was incubated with placental BeWo cells in competition with ^{59}Fe-radiolabeled Fe_2-hTF. Competitions between ^{59}Fe-hTF and Bi_2-hTF, Ga_2-hTF, Fe_2-hTF, and apo-hTF were also studied for comparison. Cell membrane-bound ^{59}Fe and intracellular ^{59}Fe were measured as described in the Experimental Section. The results are shown in Figure 8. As expected, Fe_2-hTF was a strong inhibitor of ^{59}Fe binding and uptake, as was Ga_2-hTF, in agreement with previous reports (*52*). Both Ti_2-hTF and Bi_2-hTF also showed marked dose-dependent inhibitory effects (Figure 8), whereas apo-hTF was the least effective.

DISCUSSION

The natural transferrin cycle for the delivery of iron to cells offers a potential strategy for drug targeting to tumor cells. Three features of transferrin chemistry point to the possibility that transferrin could deliver antitumor metal complexes to cancer cells. First, it is known that malignant cells have a high iron requirement and consequently express a greatly elevated level of transferrin receptors (*27*−*30*, *53*). Second, measurements of pH in vivo have shown that the microenvironment of tumors is more acidic than in normal tissue (*54*), which may facilitate Ti^{IV} release in tumor tissues. Third, although iron(III) is the natural metal ion bound by transferrins, many other metal ions can also bind at the same specific sites (*34*, *35*, *55*). In blood plasma, less than 30% of the iron sites in human transferrin are occupied by iron, and the vacant sites could be used to transport other metal ions as well. Indeed, transferrin has already been shown to be responsible for the selective delivery of $^{67}Ga^{III}$ complexes to tumor cells (*56*), and it is possible that the specific delivery of antitumor Ti^{IV} complexes can be achieved by a similar process.

Complexation of metal ions to the phenolic oxygen of the tyrosine residues in the specific metal-binding sites of apo-hTF (Chart 1) perturbs the $\pi-\pi^*$ transitions of the aromatic rings and leads to the production of two new absorption bands near 241 and 295 nm (*35*, *36*). These new bands are readily apparent in the difference UV spectra of metal-hTF and apo-hTF. Specific binding by some metal ions, such as Fe^{III}, Ce^{IV}, and Cu^{II}, also gives rise to LMCT bands in the visible region (*35*, *36*). This provides a convenient way to detect specific metal−hTF binding and release by UV−Vis spectroscopy.

The changes in the UV spectrum of hTF on reaction with Cp_2TiCl_2 are very similar to those observed previously for the binding of other metal ions to the specific Fe^{III} sites (*35*, *36*). The two sharp new bands near 242 and 295 nm are typical of phenolate groups ($\pi-\pi^*$ transitions) generated by binding of metal ions to Tyr residues in the specific iron-binding sites. The third broad band centered near 321 nm, lies in the range typical of LMCT transitions of Ti^{IV} with phenolate ligands (*57*, *58*). For example, we have observed similar bands for Ti^{IV}-EHPG (EHPG, *N*,*N*′-ethylenebis(*o*-hydroxyphenyl)glycine) model complexes with known X-ray crystal structures (*57*). The magnitude of the extinction coefficient of this LMCT band ($\Delta\epsilon_{321} = 4830\ M^{-1}\ cm^{-1}$) in physiological buffer is similar to those for Fe^{III}_2-hTF ($\Delta\epsilon_{465} = 4950\ M^{-1}\ cm^{-1}$) (*59*) and Ce^{IV}-hLF ($\Delta\epsilon_{442} = 4640\ M^{-1}\ cm^{-1}$) (*60*). The titration curve obtained by monitoring the absorbance change at 321 nm gave a sharp break at a ratio of Ti/hTF of 2:1. The same ratio was also obtained by ICP-AES measurement of bound metal (data not shown), suggesting that Ti^{IV} binds to the specific metal-binding sites in both the N-lobe and the C-lobe of the protein and that two tyrosines are involved in binding Ti^{IV} in both lobes (Tyr-95/Tyr-188 in the N-lobe and Tyr-426/Try-517 in the C-lobe) as is the case for Fe^{III} (*35*, *36*). Moreover, the displacement of Ti^{IV} from transferrin by Fe^{III} provides further evidence for specific binding of Ti^{IV} to the two lobes of the protein.

The rapid uptake of Ti^{IV} from the anticancer agent Cp_2TiCl_2 by human transferrin under physiological conditions (within 5 min in physiological buffer at 25 μM hTF, 310 K) may be relevant to its anticancer activity. Other Ti^{IV} complexes such as Ti^{IV}-citrate can also donate Ti^{IV} to hTF but very slowly (>10 h for completion under similar conditions) (*20*), while Ti^{IV}-NTA is not able to denote Ti^{IV} to transferrin (*22*).

^{1}H NMR spectroscopy shows that the cyclopentadienyl ligands are displaced from Ti^{IV} after reaction of Cp_2TiCl_2 with hTF (Figure S2 in the Supporting Information). It is known that the chloride ligands are readily displaced from Cp_2TiCl_2 in aqueous solution (e.g., by H_2O/OH on hydrolysis in water) (*7*, *13*, *19*), and therefore only the Ti^{IV} ion from the drug is taken up by the protein. It had been suggested that the active antitumor species could be the cyclopentadiene released during the decomposition of titanocene compounds (*61*). However, subsequent in vivo experiments have shown that neither cyclopentadiene (C_5H_6) nor its dimer are the active antiproliferative agents (*62*). The active component must be Ti^{IV} itself. The role of the Cp ligands may be to stabilize Ti^{IV} and prevent rapid hydrolysis to give inactive polymeric species. Thus, it may not be surprising that structurally distinct Ti^{IV} species, such as titanocene dichloride and Budotitane, share similar patterns of antitumor activity and organ toxicity (*4*, *5*).

The structural changes in hTF induced by Ti^{IV} binding were monitored by ^{1}H NMR. Resonances for apo-hTF and Ti-hTF are in slow exchange on the NMR time scale, indicative of strong Ti^{IV} binding. Resonances in the glycan region (2.0−2.1 ppm) were perturbed only on the addition of the first mole equivalent of Cp_2TiCl_2, suggesting that preferential binding of Ti^{IV} occurs to the C-lobe of hTF since the glycan chains are present only in the C-lobe. This conclusion was further confirmed by 2D HSQC NMR data using ϵ-^{13}C-Met-labeled protein. A similar NMR behavior has been observed for Ga^{III}, In^{III}, and Bi^{III} binding to hTF with bicarbonate as the synergistic anion (*46*, *47*, *63*).

The ^{13}C NMR studies showed a decrease in intensity of the peak for free (bi)carbonate and a gradual increase in intensity of the new signal at 166.5 ppm after addition of the first and second mole equivalent of Cp_2TiCl_2. This suggests that Ti^{IV} binds to both the N- and C-lobes of hTF concomitantly with carbonate as synergistic anion. The chemical shift of this bound anion is close to that observed previously for other metallo-transferrins, e.g., 166.0/166.2 ppm for Tl^{III} (*64*), 165.4 ppm for Al^{III}, 166.5 ppm for Ga^{III} (*48*), 166.8/167.2 ppm for Sc^{III} (*65*), and 165.8 ppm for Bi^{III} (*46*), suggesting a similar mode of carbonate binding, probably as a bidentate carbonate ion.

The weakness and gradual disappearance of the peak for bound carbonate suggests that Ti^{IV} binding does not require carbonate as an obligatory synergistic anion. Such a binding mode is known for VO^{2+} (*66*). The UV−Vis and NMR experiments carried out in the absence of bicarbonate reveal that Ti^{IV} can still bind to hTF at the Fe^{III} sites but in a slightly different manner. In the absence of bicarbonate, the structural changes in hTF induced by Ti^{IV} are different from those in the presence of bicarbonate, as evidenced by the ^{1}H NMR data. Chemical exchange effects could give rise to the broadening that decreases the intensity of the ^{13}C peak for bound carbonate. Such effects could arise from multiple conformations of bound carbonate as suggested from the X-ray crystal structure of recombinant N-lobe of transferrin (*67*). Ti^{IV} bound to transferrin could adopt a seven-coordinate geometry. This is favored, for example, in model complexes of Ti^{IV} with the model ligand EHPG, in which Ti^{IV} has pentagonal bipyramidal geometry with axial phenolate ligands, two amine nitrogens, two carboxylate oxygens, and an additional H_2O ligand in the equatorial plane (*57*).

The 2D [^{1}H, ^{13}C] HSQC NMR experiments on ϵ-[$^{13}CH_3$]-Met-hTF show that Ti^{IV} preferentially loads the C-lobe, followed by the N-lobe. A similar preference has been observed previously for reactions of hTF with NTA complexes of Fe^{III}, Sc^{III}, and Bi^{III} with bicarbonate as the synergistic anion (*49*). This preference can sometimes be switched by changing the initial ligands on the loading metal, but the factors that determine the preference are not well understood. The overall changes in chemical shifts for the nine Met CH_3 cross-peaks induced by Ti^{IV} are similar to those induced by Fe^{III} binding [added as $Fe(NTA)_2$], suggesting that Ti^{IV}-induced conformational changes in hTF are similar to those induced by Fe^{III} binding. This could be important for the recognition of the protein by the transferrin receptor on cell membranes and the subsequent uptake of transferrin into cells. It is known that only holo-hTF but not apo-hTF binds strongly to the receptor and is taken up into cells (*72*).

In terms of "HSAB (hard−soft−acid−base)" theory (*68*), Ti^{IV} is a "hard" Lewis acid similar to Fe^{III} and readily hydrolyzes to form insoluble polymeric species at neutral pH values. Both Cp_2TiCl_2 and Budotitane undergo rapid hydrolysis to give anticancer inactive polymeric species at neutral pH (*1*, *2*, *17*). Hence, it is likely that Ti^{IV} is stabilized by binding to certain biomolecules and is transported to the nucleus inside tumor cells. Transferrin is a strong candidate to act as mediator for the uptake of Ti^{IV} from Cp_2TiCl_2 in blood plasma and transport it to tumor cells. Both in vivo (rat) and in vitro studies using radiolabeled $^{45}Ti^{IV}$-DTPA (DTPA, diethylene-triaminepentaacetic acid) have also suggested that $^{45}Ti^{IV}$ is mainly associated with transferrin in blood plasma, and ^{45}Ti is transferred into tumor tissue over a period of 3−6 h postinjection in tumor-bearing rats (*11*).

We investigated whether Ti^{IV} can be released from Ti_2-hTF under physiologically relevant conditions. Our UV−Vis experiments showed that Ti_2-hTF is stable over the pH range of 5.0−9.5 in 100 mM NaCl, 25 mM $NaHCO_3$, 4 mM NaH_2PO_4, conditions that mimic extracellular ones. Only 53% of bound Ti^{IV} was released from transferrin even at pH 2 over a period of 1 h at 298 K. In contrast, more than 80% of Fe^{III} is released from Fe_2-hTF over the pH range 6.0 to 4.0 in the absence of chelators (*35*, *60*). Protonation of carbonate (synergistic anion) may therefore trigger Fe^{III} release but not Ti^{IV} release. However, upon introduction of ATP (at a concentration of 1 mM, a 40-fold molar excess over hTF), Ti^{IV} was readily released over the pH range of 7.0−5.0, with 50% Ti^{IV} release at pH 6.3 and almost complete release by pH 4.5. Extracellular ATP levels are low but intracellular concentrations of ATP are as high as 3−5 mM (*69*, *70*). Inside endosomes, where Fe^{III} is released, the pH is as low as 5.0−5.5 (*33*, *34*). Therefore, the release of Ti^{IV} after cellular uptake may be favored there. The ^{31}P NMR studies suggested that the γ-phosphate group of ATP was hydrolyzed after interaction of ATP with Ti_2-hTF, a reaction that is also observable for Ti^{IV}-ATP alone (*16*), suggesting that the released Ti^{IV} binds to the chelator ATP. Ti^{IV} transfer from the model ligand EHPG to ATP readily occurs at low pH or high ATP concentrations (*71*). Fe^{III} is likely to bind to ATP after it is released from transferrin in endosomes (*37*). ATP is known to be a metal macrochelator and a major intracellular iron carrier (*72*, *73*). It plays a major role in the transport of Fe^{III} to the nucleus, and the γ-phosphate of ATP is hydrolyzed during Fe^{III} transport (*73*).

Therefore ATP could also facilitate the intracellular transport of Ti^{IV} and allow it to target polynucleotides, which are condensed in the nucleus. DNA in the nucleus has a high negative charge and potentially a markedly lower pH value near its surface (up to 3 pH units lower than the bulk pH) (*74*). These factors may favor Ti^{IV} binding. Our results with nucleotides reveal that Ti^{IV} has a high affinity for O-sites of the phosphate groups and N-sites of bases at low pH (*16*). Ti-DNA adducts have been detected recently in vitro and in tumor cells treated with Cp_2TiCl_2 (*6*, *75*). Köpf and co-workers have shown that Ti^{IV} accumulates mainly in nucleic acid-rich regions of tumor cells, especially the nucleus, after both in vivo and in vitro administration of Cp_2TiCl_2 (*14*, *15*).

The UV−visible, ICP-AES, and 2D HSQC NMR data show that Fe^{III} can displace Ti^{IV} from Ti_2-hTF and that displacement of Ti^{IV} occurs preferentially and more rapidly from the C-lobe than from the N-lobe. Early studies also noted that Fe^{III} displaced one of the two Cr^{III} ions from bound transferrin or lactoferrin much more readily (*76*, *77*), but the lobe preference was not determined. There are few other reported data on lobe-selective metal displacement from hTF with which to compare, but it is interesting to note that the C-lobe is less flexible (can open only to about 75% of the N-lobe) due to the presence of an extra disulfide bridge (*35*, *36*), and metal in the N-lobe is normally more exposed and accessible (*35*). The preferential displacement of Ti^{IV} from the C-lobe of Ti_2-hTF was therefore unexpected. This could suggest that the C-site is better optimized for binding specifically to Fe^{III}. The Fe^{III} loaded C-lobe appears to be responsible for receptor recognition (*23*, *24*, *34*). The cross-peaks for the N-lobe Met residues were affected by the addition of the second mole equivalent of Fe^{III}. The displacement of Ti^{IV} from the N-lobe was very slow, but Fe_2-hTF was finally formed after 3 d (Figure 6). A new cross-peak for an unassigned Met residue appeared during substitution of the C-lobe Ti^{IV} by Fe^{III}, a peak not present in spectra of Ti_2-hTF or Fe_2-hTF (peak marked by an asterisk in Figure 6). This may represent an intermediate in which the C-lobe/N-lobe interface is perturbed. Additional evidence for this mechanism was provided by the shift of the Fe^{III}-hTF LMCT band [ca. 470 nm for Fe_2-hTF, an average for N- and C-lobes and 473 nm for the N-lobe alone (*35*, *78*)] during the two-phase of Fe^{III} displacement Ti^{IV} from Ti_2-hTF (Figure S6). The absorption maximum of the LMCT band shifted from 465 nm in the first fast phase to 472 nm in the second slow phase, suggesting that metal displacement occurs in the C-lobe first followed by the N-lobe. The two-phase displacement was further confirmed by ICP-AES measurement of protein metal content during the reaction course (Figure 7). The two-phase displacement implies that Fe_CTi_N-hTF could survive for a long time (days) under physiological conditions. Because the primary receptor recognition sites on human transferrin appear to be in the C-lobe (*23*−*25*, *35*), hTF with Fe^{III} in the C-lobe and Ti^{IV} in the N-lobe (Fe_CTi_N-hTF) may be recognized by the transferrin receptor and taken up into cells. Therefore, the formation of both Ti_2-hTF and Fe_CTi_N-hTF may provide routes for entry of Ti^{IV} into cells.

The cell uptake experiments show that Ti_2-hTF competes with Fe_2-hTF for membrane binding and uptake into BeWo cells, although it is slightly less effective than Ga_2-hTF, which has previously been shown to enter cells via the transferrin receptor (*52*, *79*). Bi_2-hTF also appears to be recognized by the transferrin receptor. Ti^{IV}, Bi^{III}, and Fe^{III} binding appear to induce similar conformational changes in hTF, as judged from the ^1H and ^{13}C NMR shift data (*46*). A recent X-ray crystal structure of Sm_2-lactoferrin has revealed that the large metal ion Sm^{3+} induces the same overall structural changes in this protein as Fe^{3+}, although different structural changes occur at the metal binding sites (*80*). Therefore, both chemical and biochemical experiments suggest that Ti^{IV} can be taken up and released inside cells via transferrin-mediated routes.

Metal anticancer agents can react with various biomolecules in vivo including carriers such as albumin, transferrin, ATP, citrate, and GSH, which communicate between extracellular and intracellular and between various intracellular compartments. Substrate binding is finely controlled by natural gradients that exist in different tissues or cellular compartments (e.g., pH, ATP, and ionic gradients). These gradients may alter the relative affinity of drug molecules for different cellular components and facilitate drug transport to their targets. "Hard" Ti^{IV} may be transported into tumor cells by transferrin and subsequently bind to DNA at both the negatively charged phosphates on the backbone and base N-donors (*13b*, *81*). The high DNA concentration in the cell nucleus, the much lower dielectric constant (*82*), and potentially the low pH close to the surface of DNA may favor DNA as a target for Ti^{IV}.

CONCLUSIONS

We have shown that Ti^{IV} from the antitumor drug Cp_2TiCl_2 is readily taken up into the two specific iron sites of human transferrin under physiological conditions, in the presence of carbonate as a synergistic anion. Both Cp^- ligands are displaced during Ti^{IV} uptake. Ti^{IV} is preferentially taken up into the C-lobe, followed by the N-lobe as indicated by NMR spectroscopy. Binding of Ti^{IV} appears to induce similar conformational changes in hTF to those induced by Fe^{III} binding in the presence of bicarbonate. Ti^{IV} can also bind to apo-hTF in the absence of bicarbonate but induces different structural changes from those in the presence of bicarbonate. Bicarbonate is readily displaced from Ti_2-hTF. ATP facilitates the release of Ti^{IV} from transferrin complexes. Unexpectedly, Fe^{III} displaces Ti^{IV} from the C-lobe more rapidly than from the N-lobe. Fe_CTi_N-hTF may be a significant species under physiological conditions and be recognized by transferrin receptors and taken up into cells. Ti_2-hTF blocked both membrane binding and cellular uptake of ^{59}Fe-hTF into BeWo placental cancer cells. The rapid and strong interaction of the anticancer drug titanocene dichloride with transferrin may be relevant to its low toxicity and high activity. It would be of interest to investigate whether transferrin can enhance the anticancer activity of titanium agents.

ACKNOWLEDGMENT

We are grateful to Dr. J. A. Parkinson (Edinburgh) for helpful advice on NMR experiments and Professor R. C. Woodworth and Dr. A. B. Mason (Department of Biochemistry, University of Vermont) for supplying samples of recombinant transferrin (supported by Grant DK-21739 to R.C.W. from the U.S. Public Health Service) and for comments on the script.

SUPPORTING INFORMATION AVAILABLE

Figure S1: Resolution-enhanced 500-MHz ^{1}H NMR spectra of hTF showing the effect of Cp_2TiCl_2 on the *N*-acetyl region. Figure S2: 500-MHz ^{1}H NMR showing the displacement of Cp from Cp_2TiCl_2 during reaction with apo-hTF. Figure S3 showing the detection of carbonate binding as synergistic anion during reaction of apo-hTF with Cp_2TiCl_2 by ^{13}C NMR (125 MHz). Figure S4 showing a comparison of the effects of Cp_2TiCl_2 on the high field region of resolution-enhanced 500-MHz ^{1}H NMR spectra of hTF in the presence and in the absence of bicarbonate. Figure S5 showing the locations of the nine Met residues in hTF. Figure S6 showing the dependence of the difference absorption spectrum of Ti_2-hTF on time after addition of 2.5 mol equiv of $Fe(NTA)_2$. This material is available free of charge via the Internet at http://pubs.acs.org.

REFERENCES

1. (a) Köpf-Maier, P., and Köpf, H. (1987) *Chem. Rev. 87*, 1137−1153, and references therein. (b) Köpf-Maier, P., and Köpf, H. (1986) *Drugs Future 11*, 297−319, and references therein. (c) Köpf-Maier, P., and Köpf, H. (1994) in *Metal Compounds in Cancer Therapy* (Fricker, S. P., Ed.) pp 109−146, Chapman & Hall, London.
2. Keppler, B. K., Friesen, C., Vongerichten, H., and Vogel, E. (1993) in *Metal Complexes in Cancer Chemotherapy* (Keppler, B. K., Ed.) pp 297−323, VCH, Weinhein.
3. (a) Sadler, P. J. (1991) *Adv. Inorg. Chem. 36*, 1−48. (b) Guo, Z., and Sadler, P. J. (1999) *Adv. Inorg. Chem. 49*, 183−305.
4. Köpf-Maier, P. (1994) *Eur. J. Clin. Pharmacol. 47*, 1−14.
5. Christodoulou, C. V., Ferry, D. R., Fyfe, D. W., Young, A., Doran, J., Sheehan, T. M. T., Eliopoulos, A. G., Hale, K., Baumgart, J., Sass, G., and Kerr, D. J. (1998) *J. Clin. Oncol. 16*, 2761−2769.
6. Christodoulou, C. V., Eliopoulos, A. G., Young, L. S., Hodgkins, L., Ferry, D. R., and Kerr, D. J. (1998) *Br. J. Cancer 77*, 2088−2097.
7. Köpf-Maier, P., and Köpf, H. (1988) *Struct. Bonding 70*, 105−185.
8. Duffy, B., Schwietert, C., France, A., Mann, N., Culbertson, K., Harmon, B., and McCue, J. P. (1998) *Biol. Trace Elem. Res. 64*, 197−213.
9. Schwietert, C., and McCue, P. J. (1999) *Coord. Chem. Rev. 184*, 67−89.
10. Tornieporth-Oetting, I. C., and White, P. S. (1995) *Organometallics 14*, 1632−1636.
11. Ishiwata, K., Ido, T., Monma, M., Murakami, H., Fukuda, M., Kammeyama, K., Yamada, K., Endo, S., Yoshioka, S., Sato, T., and Matsuzawa, T. (1991) *Appl. Radiat. Isot. 42*, 707−712.
12. (a) Jamieson, E. J., and Lippard, S. J. (1999) *Chem. Rev. 99*, 2467−2498. (b) Reedijk, J. (1999) *Chem. Rev. 99*, 2499−2510. (c) Guo, Z., and Sadler, P. J. (1999) *Angew. Chem., Int. Ed. Engl. 38*, 4001−4019, and references therein.
13. (a) Kuo, L. Y., Liu, A. H., and Marks, T. J. (1996) *Met. Ions Biol. Sys. 33*, 53−85. (b) Yang, P., and Guo, M. L. (1999) *Coord. Chem. Rev. 186*, 189−211, and references therein.
14. Köpf-Maier, P., and Martin, R. (1989) *Virchows Arch. B Cell Pathol. 57*, 213−222.
15. Köpf-Maier, P. (1990) *J. Struct. Biol. 105*, 35−45.
16. Guo, M. L., and Sadler, P. J., unpublished results.
17. Toney, J. H., Brock, C. P., and Marks, T. J. (1986) *J. Am. Chem. Soc. 108*, 7263−7274.
18. Harding, M. M., Mokdsi, G., Mackay, J. P., Prodigalidad, M., and Lucas, S. W. (1998) *Inorg. Chem. 37*, 2432−2437.
19. Toney, J. H., and Marks, T. J. (1985) *J. Am. Chem. Soc. 107*, 947−953.
20. Sun, H., Li, H., Weir, R., and Sadler, P. J. (1998) *Angew. Chem., Int. Ed. Engl. 37*, 1577−1579.
21. Guo, M. L., Sun, H., and Sadler, P. J. (1999) *J. Inorg. Biochem. 74*, 150.
22. Messori, L., Orioli, P., Banholzer, V., Pais, I., and Zatta, P. (1999) *FEBS Lett. 442*, 157−161.
23. (a) Bali, P. K., and Aisen, P. (1991) *Biochemistry 30*, 9947−9952. (b) Zak, O., Trinder, D., and Aisen, P. (1994) *J. Biol. Chem. 269*, 7110−7114.
24. Mason, A. B., Tam, B. M., Woodworth, R. C., Oliver, R. W. A., Green, B. N., Lin, L. N., Brandts, J. F., Savage, K. J., Lineback, J. A., and MacGillivray, R. T. A. (1997) *Biochem. J. 326*, 77−85.
25. Lawrence, C. M., Ray, S., Babyonyshev, M., Galluser, R., Borhani, D. W., and Harrison, S. C. (1999) *Science 286*, 779−782.
26. Wagner, E., Curiel, D., and Cotten, M. (1994) *Adv. Drug Delivery Rev. 14*, 113−135 and references therein.
27. Flulk, W. P., Hsi, B. L., and Stevens, P. J. (1980) *Lancet 2*, 390−392.
28. Yeh, C. J. G., Taylor, C. G., and Faulk, W. P. (1984) *Vox Sang. 46*, 217−223.
29. Panaccio, M., Zalcberg, J. R., Thompson, C. H., Leyden, M. J., Sullivan, J. R., Lichtenstein, M., and McKenzie, I. F. (1987) *Immunol. Cell Biol. 65*, 461−472.
30. Seymour, G. J., Walsh, M. D., Lavin, M. F., Strutton, G., and Gardiner, R. A. (1987) *Urol. Res. 15*, 341−344.
31. Chitambar, C. R., Matthaeus, W. G., Antholine, W. E., Graff, K., and O'Brien, W. J. (1988) *Blood 72*, 1930−1938.
32. Kratz, F., Hartmann, M., Keppler, B. K., and Messori, L. (1994) *J. Biol. Chem. 269*, 2581−2588.
33. (a) Klausner, R. D., Ashwell, G., Harford, J. B., and Bridges, K. R. (1983) *Proc. Natl. Acad. Sci. U.S.A. 80*, 2263−2266. (b) Klausner, R. D., van Renswoude, J., Ashwell, G., Kempf, C., Schechter, A. N., Dean, A., and Bridges, K. R. (1983) *J. Biol. Chem. 258*, 4715−4724. (c) Dautry-Varsat, A., Ciechanover, A., and Lodish, H. F. (1983) *Proc. Natl. Acad. Sci. U.S.A. 80*, 2263−2266. (d) Ciechanover, A., Schwartz, A. L., Dautry-Varsat, A., and Lodish, H. F. (1983) *J. Biol. Chem. 258*, 9681−9689. (e) Hopkins, C. R., and Trowbridge, I. S. (1983) *J. Cell Biol. Chem. 97*, 506−521.
34. Aisen, P. (1998) *Met. Ions Biol. Sys. 35*, 585−631, and references therein.
35. Baker, E. N. (1994) *Adv. Inorg. Chem. 41*, 389−463, and references therein.
36. Sun, H., Li, H., and Sadler, P. J. (1999) *Chem. Rev. 99*, 2817−2842, and references therein.
37. (a) Weaver, J., and Pollack, S. (1989) *Biochem. J. 261*, 789−792. (b) Weaver, J., Zhan, H., and Pollack, S. (1993) *Br. J. Haematol. 83*, 138−144.
38. Mason, A. B., Miller, M. K., Funk, W. D., Banfield, D. K., Savage, K. L., Oliver, R. W. A., Green, B. N., MacGillivray, R. T. A., and Woodworth, R. C. (1993) *Biochemistry 32*, 5472−5479.
39. Beatty, E. J., Cox, M. C., Frenkiel, T. A., Tam, B. M., Mason, A. B., MacGillivray, R. T. A., Sadler, P. J., and Woodworth, R. C. (1996) *Biochemistry 35*, 7635−7642.
40. Chasteen, N. D., White, L. K., and Campbell, R. F. (1977) *Biochemistry 16*, 363−368.
41. Bax, A., Griffey, R. H., and Hawkins, B. L. (1983) *J. Magn. Reson. 55*, 301−315.
42. Shaka, A. J., Barker, P. B., and Freeman, R. (1985) *J. Magn. Reson. 64*, 547−522.
43. McArdle, H. J., Douglas, A. J., Bowen, B. J., and Morgan, E. H. (1985) *J. Cell. Physiology 124*, 446−450.
44. Sun, H., Cox, M. C., Li, H., and Sadler, P. J. (1997) *Struct. Bonding 88*, 71−102.
45. Lu, J., and van Halbeek, H. (1996) *Carbohydr. Res. 296*, 1−21.
46. (a) Li, H., Sadler, P. J., and Sun, H. (1996) *J. Biol. Chem. 271*, 9483−9489. (b) Sun, H., Li, H., Mason, A. B., Woodworth, R. C., and Sadler, P. J. (1999) *Biochem. J. 337*, 105−111.
47. Kubal, G., Mason, A. B., Sadler, P. J., Tucker, A., and Woodworth, R. C. (1992) *Biochem. J. 285*, 711−714.
48. Bertini, I., Luchinat, C., Messori, L., Scozzafava, A., Pellacani, G. C., and Sola, M. (1986) *Inorg. Chem. 25*, 1782−1786.

49. Sun, H., Cox, M. C., Li, H., Mason, A. B., Woodworth, R. C., and Sadler, P. J. (1998) *FEBS Lett. 22*, 315−320.
50. He, Q. Y., Mason, A. B., Tam, B. M., MacGillivray, R. T. A., and Woodworth, R. C. (1999) *Biochem. J. 344*, 881−887.
51. Korn, S., and Sheldrick, W. S. (1997) *J. Chem. Soc., Dalton Trans.* 2191−2199.
52. Chitambar, C. R., and Narasimhan, J. (1991) *Pathobiology* 59, 3−10.
53. Cazzola, M., Bergamaschi, G., Dezza, L., and Arosio, P. (1990) *Blood 75*, 1903−1919.
54. Yamagata, M., and Tannock, I. F. (1996) *Br. J. Cancer 73*, 1328−1334.
55. Smith, C. A., Sutherland-Smith, A. J., Keppler, B. K., Kratz, F., and Baker, E. N. (1996) *J. Biol. Inorg. Chem. 1*, 424−431.
56. Ward, S. G., Taylor, R. C. (1988) in *Metal-Based Antitumour Drugs* (Gielen, M. F., Ed.) pp 1−54, Freund, London.
57. Guo, M. L., Sun, H., Bihari, S., Parkinson, J. A., Gould, R. O., Parsons, S., and Sadler, P. J. (2000) *Inorg. Chem. 39*, 206−215.
58. Harrod, J. F., and Taylor, K. R. (1975) *Inorg. Chem. 14*, 1541−1545.
59. Bali, P. K., and Harris, W. R. (1990) *Arch. Biochem. Biophys. 281*, 251−256.
60. Smith, C. A., Ainscough, E. W., Baker, H. M., Brodie, A. M., and Baker, E. N. (1994) *J. Am. Chem. Soc. 116*, 7889−7890.
61. Döppert, K. (1987) *J. Organomet. Chem. 319*, 351−354.
62. Köpf-Maier, P., and Köpf, H. (1988) *J. Organomet. Chem. 342*, 167−176.
63. Beatty, E. J. (1995) Recognition of Metal Ions and Anions by the N-lobe of Human Serum Transferrin, Ph.D. Thesis, University of London.
64. Aramini, J. M., Krygaman, P. H., and Vogel, H. J. (1994) *Biochemistry 33*, 3304−3311.
65. Aramini, J. M., and Vogel, H. J. (1994) *J. Am. Chem. Soc. 116*, 1988−1993.
66. Saponja, J. A., and Vogel, H. J. (1996) *J. Inorg. Biochem. 62*, 253−270.
67. MacGillivray, R. T. A., Moore, S. A., Chen, J., Anderson, B. F., Baker, H., Luo, Y., Bewey, M. C., Smith, C. A., Murphy, M. E. P., Mason, A. B., Woodworth, R. C., Brayer, G. D., and Baker, E. N. (1998) *Biochemistry 37*, 7919−7928.
68. Pearson, R. G. (1969) in *Survey of Progress in Chemistry* (Scott, A., Ed.) Chapter 1, Academic Press, New York.
69. Mathews, C. K., and van Holde, K. E. (1990) *Biochemistry*, pp 410, Benjamin/Cummings Pub. Co. Inc., Redwood City, CA.
70. Hatakeyama, K., Harada, T., and Kagamiyama, H. (1992) *J. Biol. Chem. 267*, 20734−20739.
71. Guo, M. L., and Sadler, P. J. (2000) *J. Chem. Soc., Dalton Trans.* 7−9.
72. Aisen, P. (1994) *Adv. Exp. Med. Biol. 356*, 31−40.
73. Gurgueira, S. A., and Meneghini, R. (1996) *J. Biol. Chem. 271*, 13616−13620.
74. Lamm, G., and Pack, G. R. (1990) *Proc. Natl. Acad. Sci. U.S.A. 87*, 9033−9036.
75. McLaughlin, M. L., Cronan, J. M., Jr., Schaller, T. R., and Sneller, R. D. (1990) *J. Am. Chem. Soc. 112*, 8949−8952.
76. Aisen, P., Aasa, R., and Redfield, A. G. (1969) *J. Biol. Chem. 244*, 4628−4633.
77. Ainscough, E. W., Brodie, A. M., Plowman, J. E., Bloor, S. J., Loehr, J. S., and Loehr, T. M. (1980) *Biochemistry 19*, 4072−4079.
78. Woodworth, R. C., Mason, A. B., Funk, W. D., and MacGillivary, R. T. A. (1991) *Biochemistry*, *30*, 10824−10829.
79. Clarke, M. J., Zhu, F., and Frasca, D. R. (1999) *Chem. Rev. 99*, 2511−2533.
80. Sharma, A. K., and Singh, T. P. (1999) *Acta Crystallogr. Sect. D 55*, 1799−1804.
81. (a) Guo, M. L., Yang, P., Yang, B. S., and Zhang, Z. Z. (1996) *Chin. Sci. Bull. 41*, 1098−1102. (b) Yang, P., and Guo, M. L. (1998) *Met.-Based Drugs 5*, 41−58.
82. (a) Lamm, G., and Pack, G. R. (1997) *J. Phys. Chem. B 101*, 959−965. (b) Jin, R., and Breslauer, K. J. (1988) *Proc. Natl. Acad. Sci. U.S.A. 85*, 8939−8942. (c) Barawkar, D. A., and Ganesh, K. N. (1995) *Nucleic Acids Res. 23*, 159−164. (d) Yang, L., Weerasinghe, S., Smith, P. E., and Pettitt, B. M. (1995) *Biophys. J. 69*, 1519−1527.

BI000798Z